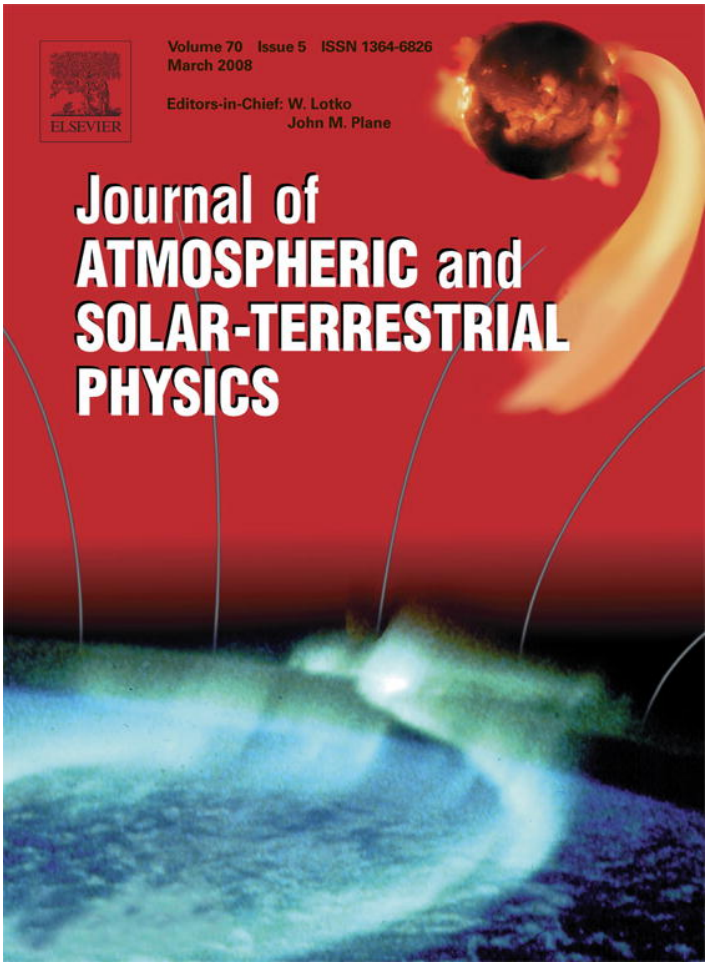

ELSEVIER

Journal of Atmospheric and Solar-Terrestrial Physics 70 (2008) 730–741

Journal of ATMOSPHERIC AND SOLAR-TERRESTRIAL PHYSICS

www.elsevier.com/locate/jastp

The northern annular mode in summer and its relation to solar activity variations in the GISS ModelE

Jae N. Lee[a,*], Sultan Hameed[a], Drew T. Shindell[b]

[a]*Institute for Terrestrial and Planetary Atmospheres, Stony Brook University, Stony Brook, NY 11794-5000, USA*
[b]*NASA Goddard Institute for Space Studies and Columbia University, New York, NY, USA*

Received 20 April 2007; received in revised form 5 October 2007; accepted 13 October 2007
Available online 19 November 2007

Abstract

The northern annular mode (NAM) has been successfully used in several studies to understand the variability of the winter atmosphere and its modulation by solar activity. The variability of summer circulation can also be described by the leading empirical orthogonal function (EOF) of geopotential heights. We compare the annular modes of the summer geopotential heights in the northern hemisphere stratosphere and troposphere in the Goddard Institute for Space Studies (GISS) ModelE with those in the National Centers for Environmental Prediction/National Center for Atmospheric Research (NCEP/NCAR) reanalysis. In the stratosphere, the summer NAM obtained from NCEP/NCAR reanalysis as well as from the ModelE simulations has the same sign throughout the northern hemisphere, but shows greater variability at low latitudes. The patterns in both analyses are consistent with the interpretation that low NAM conditions represent an enhancement of the seasonal difference between the summer and the annual averages of geopotential height, temperature and velocity distributions, while the reverse holds for high NAM conditions. Composite analysis of high and low NAM cases in both model and observation suggests that the summer stratosphere is more ''summer-like'' when the solar activity is near a maximum. This means that the zonal easterly wind flow is stronger and the temperature is higher than normal. Thus increased irradiance favors a low summer NAM. A quantitative comparison of the anti-correlation between the NAM and the solar forcing is presented in the model and in the observation, both of which show lower/higher NAM index in solar maximum/minimum conditions. The temperature fluctuations in simulated solar minimum conditions are greater than in solar maximum throughout the summer stratosphere.

The summer NAM in the troposphere obtained from NCEP/NCAR reanalysis has a dipolar zonal structure with maximum variability over the Asian monsoon region. The corresponding EOF in ModelE has a qualitatively similar structure but with less variability in the Asian monsoon region which is displaced eastward of its observed position. In both the NCEP/NCAR reanalysis and the GCM the negative anomalies associated with the NAM in the Euro-Atlantic and Aleutian island regions are enhanced in the solar minimum conditions, though the results are not statistically significant.

Keywords: Stratosphere; Troposphere; Summer northern annular mode; Solar activity

*Corresponding author. Tel.: +1 631 632 3191.
E-mail address: jaelee@atmsci.msrc.sunysb.edu (J.N. Lee).

1364-6826/$ - see front matter
doi:10.1016/j.jastp.2007.10.012

1. Introduction

The absorption of solar ultraviolet (UV) radiation by ozone creates heating in the stratosphere. Heating maximizes in the polar region in summer, and this creates a meridional temperature gradient that induces an easterly jet. Wagner and Bowman (2000) calculated the Eliassen–Palm flux vectors using the UKMO stratospheric analysis and showed that wave activity propagates vertically into the stratosphere in the presence of easterly winds during the summer time. This suggests that stratospheric dynamics in the summer is not entirely dependent on radiative forcing but is influenced by interaction with atmospheric waves propagating up to the stratosphere.

Recently, Lee and Hameed (2007) investigated the northern annular mode (NAM) in the summer geopotential heights in the stratosphere and troposphere using National Centers for Environmental Prediction/National Center for Atmospheric Research (NCEP/NCAR) reanalysis data. Considering the first Empirical Orthogonal Function (EOF) of 10 hPa geopotential heights for 1948–2004, they showed that the structure of the summer NAM in the stratosphere is different from that of the winter NAM. The summer NAM pattern has the same sign everywhere but greater variability at low latitudes. The summer NAM pattern in the stratosphere affords a physically consistent interpretation in that the low NAM represents an enhancement of the average summer condition and the high NAM represents a weakening of the average summer condition. In the less summer-like conditions characteristic of high NAM, the temperature is colder, the easterly zonal circulation is weaker and the meridional gradient of geopotential height is more negative than average summer conditions. Lee and Hameed (2007) also showed that the principal components of the first EOF in the stratosphere and upper troposphere are inversely correlated with the solar UV flux, i.e., in solar maximum conditions the stratospheric circulation is more summer-like than average and the NAM index is low, while in the solar minimum case, it is less summer-like and the NAM index is high. The purpose of this paper is to investigate the summer NAM in the stratosphere and in the troposphere and its response to the solar activity from the ModelE version of the Goddard Institute for Space Studies (GISS) atmospheric general circulation model (GCM). In the previous work of Lee and Hameed (2007), the NAM correlation with the solar activity was found from a time series analysis of the NCEP/NCAR reanalysis. We now compare estimates of the NAM index response to solar forcing in the model experiments with NAM index changes due to the solar cycle derived from the reanalysis. This allows us to better understand the physical causes and significance of the apparent summer correlation between solar output and the NAM.

2. Model description and experiment setup

The GISS ModelE simulations are performed separately for two solar activity conditions: solar maximum and solar minimum. The simulations are forced with an 11-year solar cycle irradiance variation. The full solar irradiance variation corresponds to $\sim$0.19 W/m^2 maximum minus minimum instantaneous radiative forcing at the tropopause, equivalent to 1.1 W/m^2 change in solar irradiance at the top of the atmosphere. The variation increases markedly at UV wavelengths, where the flux changes by several percent over a solar cycle (the total irradiance variation is only about 0.1%). The spectrally varying solar irradiance perturbation inputted to the three-dimensional chemistry-coupled atmospheric GCM produces stratospheric and tropospheric ozone changes (Shindell et al., 2006a).

The GISS atmospheric GCM used in this study is coupled to a simplified thermodynamic mixed-layer ocean model, where the SST is allowed to adjust to different atmospheric fluxes but the ocean heat transport is held constant. The oceanic heat convergence (the q-fluxes) into the isothermal mixed layer is calculated as a residual given by the heat and mass fluxes at the base of the atmosphere and observed mixed layer temperature and depth. The 23-layer version of ModelE resolves the stratosphere, extending from the surface to 0.02 hPa, and includes a parameterization of gravity-wave drag. The GCM output is given on a 4° (latitude) × 5° (longitude) grid. Further details on the model are given by Schmidt et al. (2006). The simulation is 37 years of equilibrium runs with present-day greenhouse gas conditions and with changes in solar irradiance under perpetual solar maximum (MAX) and perpetual solar minimum (MIN) conditions, respectively. The same coupled composition–climate atmospheric model has recently been used in similar solar simulations, but including a coupled dynamic ocean, that explored the response of tropical hydrology to persistent solar forcing (Shindell et al., 2006b).

3. Method

For the calculation of the NAM (Baldwin and Dunkerton, 2001) from the simulated geopotential heights, the same EOF analysis is used as described in Lee and Hameed (2007). To define the summer annular mode at each of the 23 pressure levels ranging from 972 to 0.017 hPa, the monthly averaged model outputs of the simulations from May to September from 20°N to 90°N are used. Data are weighted by the square root of cosine of latitude to generate the equal area weight at each grid points. Month to month variability of the leading mode is calculated at each pressure level for the extended summer season by projecting the monthly geopotential height anomalies onto the leading EOF patterns. The principal components of the leading EOF of geopotential heights are stabilized after the first 20 years of simulation at stratospheric pressure levels. For this reason, the analysis presented in this paper is for the last 17 years from the 37 years of MAX and MIN simulation. Besides the model outputs, we also employ the 1948–2004 data from the NCEP/NCAR reanalysis (Kalnay et al., 1996). The data include monthly averages of geopotential height, zonal wind and temperature fields on a 2.5° (latitude) × 2.5° (longitude) grid at 17 vertical pressure levels ranging from 1000 to 10 hPa.

4. Structure of the summer NAMs in ModelE compared with NCEP/NCAR

The first EOF patterns of geopotential height anomalies in the upper stratosphere from May to September, defined as the summer NAM, are shown in Fig. 1. In the GISS ModelE output, the summer NAM explains about 41% of the total variance of the domain, while the corresponding fraction is 73% for the reanalysis. Nevertheless, the spatial structure of the leading mode derived from the model simulation appears remarkably similar to that from the observations. For both the model and the reanalysis, the summer mode is characterized by a large degree of zonal symmetry and by the amplitude being highest in the tropics and monotonically decreasing towards the higher latitudes. We define the polarity of the principal component at this level as positive (high NAM) for an accentuation of the pattern which represents the rapid decrease of geopotential height from the polar cap towards the tropics.

In the troposphere, the model does not produce coherent EOF patterns near the surface. This may reflect distortion of the height field due to poor representation of boundary layer fluxes in the model or the strong influence of topography in the relatively coarse model grid, despite the model's use of sigma levels in the troposphere. The lowest level at which a coherent EOF pattern is obtained is 765 hPa, and it is compared with the NCEP/NCAR EOF at 850 hPa in Fig. 2. In each dataset, the pattern is characterized by a dipole zonal structure like the winter NAM which describes a zonal circulation around the polar vortex and meridional contrast between the high latitudes and the mid-latitudes. With the highest amplitudes of variability in the Atlantic basin and Europe, this leading EOF

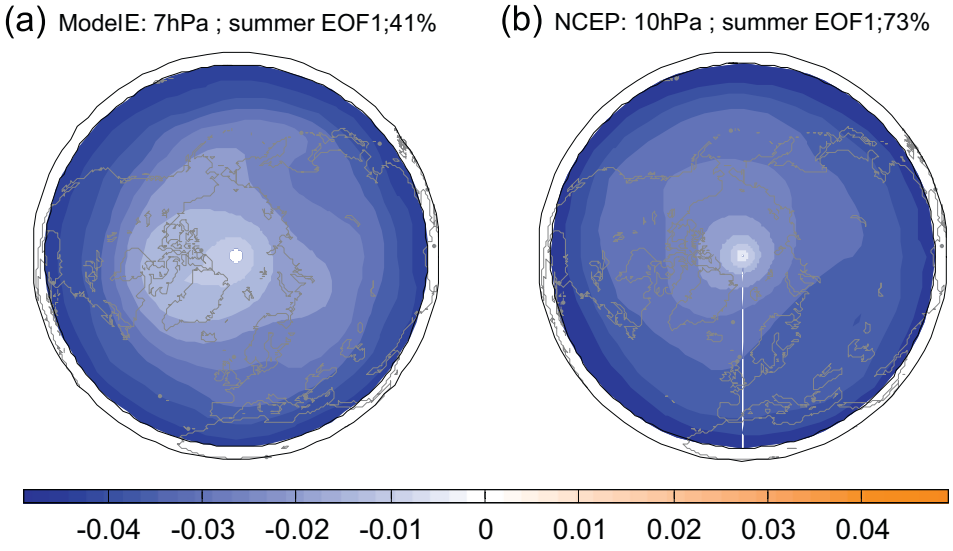

Fig. 1. NAM patterns for summer (from May to September) for (a) the GISS ModelE run at 7 hPa (left) and for (b) NCEP/NCAR reanalysis at 10 hPa (right). The patterns are calculated as the first EOFs of monthly geopotential height anomalies from 20°N to 90°N.

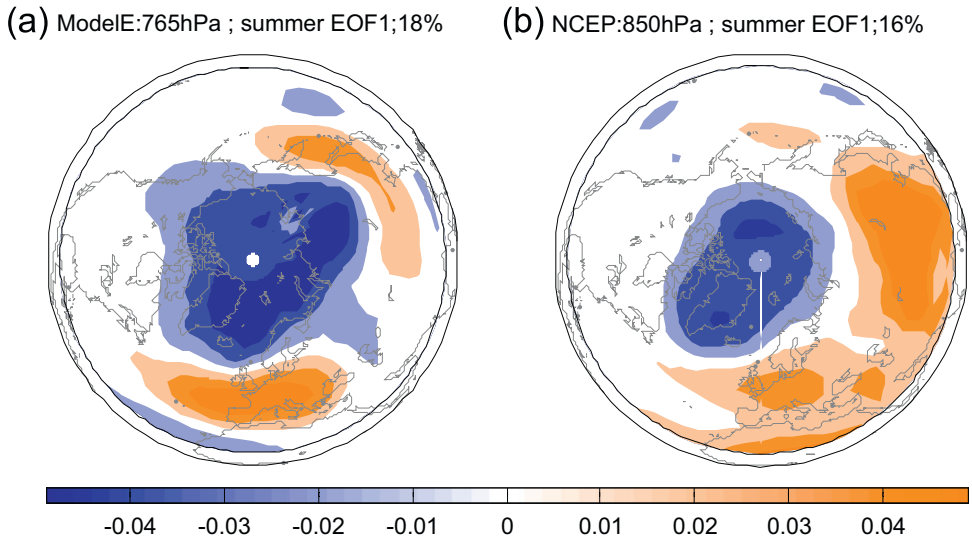

Fig. 2. NAM patterns for summer (from May to September) for (a) GISS ModelE run at 765 hPa (left) and for (b) NCEP/NCAR reanalysis at 850 hPa (right). The patterns are calculated as the first EOFs of monthly geopotential height anomalies from 20°N to 90°N.

pattern of ModelE is similar to the North Atlantic Oscillation signature. Compared with the first EOF pattern of NCEP/NCAR reanalysis, the dominant positive center of action over Asia in the ModelE is shifted towards the east. This suggests that the Asian summer monsoon simulated in the ModelE is weaker than that in NCEP/NCAR, and its region of maximum intensity is displaced to the east. The first summer mode explains 18% (16%) of the variance in the ModelE (NCEP/NCAR) in the domain at this level. Overall, the first summer mode in the troposphere derived from the ModelE appears broadly similar to that of the observations in both structure and amplitude.

5. Sun–climate coupling during summer in GISS/ModelE

Dynamic coupling between the stratosphere and the troposphere is expected to be reduced in summer compared with winter due to the dominating easterlies in the summer stratosphere, which obstruct the vertical propagation of planetary waves (Charney and Drazin, 1961). Therefore, solar-induced circulation anomalies in the middle atmosphere are less likely to be amplified by the planetary-scale Rossby waves and propagated downward through the stratosphere in comparison with the winter season.

On the other hand, the sun–middle atmosphere connection could be enhanced in summer via sun–ozone interactions, due to the migration of the summer hemisphere towards the sun. The prolonged UV irradiation input to the summer hemisphere not only produces more ozone in the stratosphere via photochemical processes, but is also absorbed by ozone, which leads to increased temperature. This radiative mechanism can amplify the solar signal in the stratosphere through a positive feedback with the ozone concentration modulated by dynamical feedbacks (Geller, 2006).

To examine this hypothesis, namely, that the solar–ozone interaction may create temperature and circulation anomalies in the upper stratosphere during the summer, the summer NAM indexes in the MAX and MIN runs are compared. But first we examine the summer NAM in the model further to see if its physical interpretation is consistent with that obtained from the NCEP/NCAR reanalysis by Lee and Hameed (2007).

5.1. *Physical significance of the summer NAM in GISS/ModelE*

The amplitude of the principal component of the first EOF at 7 hPa is called the NAM index in the discussion below. For composite analysis, high NAM index months are then defined as those in which its value is above one standard deviation from the mean of the 17 years outputs (12 months for MAX run and 16 months for MIN run). The low NAM index months are similarly defined as those in which it is below one standard deviation (11 months for MAX run and 14 months for MIN run).

In Fig. 3, the geopotential height fields at 7 hPa between low and high NAM conditions are

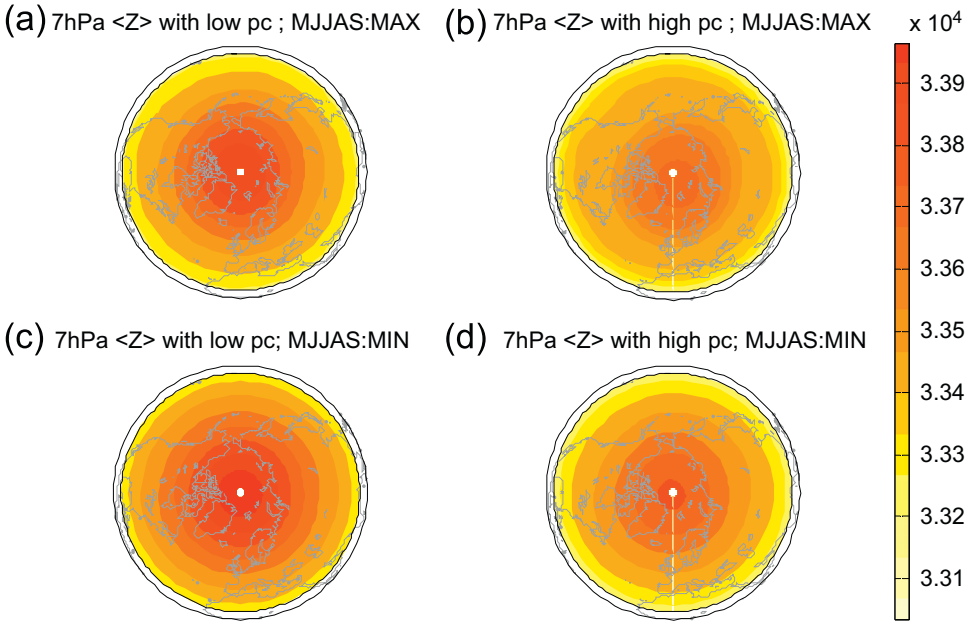

Fig. 3. Composites of geopotential height fields from GISS ModelE MAX and MIN simulations for low NAM index (left) and high NAM index (right) at 7 hPa from May to September. For the low NAM composites, 11 months for MAX run and 14 months for MIN run are averaged in (a) and (c), respectively. For the high NAM composites, 12 months for MAX run and 16 months for MIN run are averaged in (b) and (d), respectively.

compared for GISS ModelE MAX and MIN runs, respectively. In the climatological mean conditions in summer, there are high temperatures over the arctic stratosphere caused by direct absorption of UV radiation in comparison with lower latitudes. The geopotential heights in the polar region are high and decrease towards the subtropics, giving the geopotential height distribution over the summer stratosphere a dome-like shape centered on the polar region.

As shown in the figure, the model analysis shows that the geopotential height is greater throughout the domain (20–90°N) when the summer NAM index is low in comparison with the high NAM condition. Moreover, the low NAM is characterized by a smaller meridional height decrease from pole to low latitudes in both runs. Thus the low NAM represents an accentuation of the mean geopotential height distribution with greater height at each location and a more dome-like structure. Similarly, the high NAM regime is characterized by negative height anomalies everywhere with respect to the mean summer state.

Lee and Hameed (2007) showed that the correlations between the UV flux and NAM index are negative, i.e., solar maximum/minimum conditions correspond to lower/higher summer NAM with the NCEP/NCAR reanalysis. In Fig. 4, the response of NAM index to the solar forcing in the model is shown and compared with those of the NCEP/NCAR reanalysis. For the ModelE, the principal components are calculated for MAX and MIN simulations as described before. For the NCEP/NCAR reanalysis, the summer months with the monthly mean UV flux (Lean, 2000) above/below one standard deviation from the mean are grouped as solar maximum/minimum (60 months/63 months). According to this criterion, the months with 290–295 nm UV flux greater/smaller than 12.26/12.15 W/m^2 are sampled as solar maximum/minimum. In both model and observation, the NAM indexes are lower in solar maximum than in the solar minimum within 99% significant level (see Table 1). The variance of the NAM index is greater in MIN than in MAX in the model, while it is greater in solar maximum than in solar minimum in the observation. The amplitude of NAM variability of the model is less than that of the NCEP/NCAR data.

5.2. *Response of the summer NAM in the stratosphere to solar variability*

The difference between the low and the high NAM composites of the geopotential height has positive height differences throughout the hemisphere in both

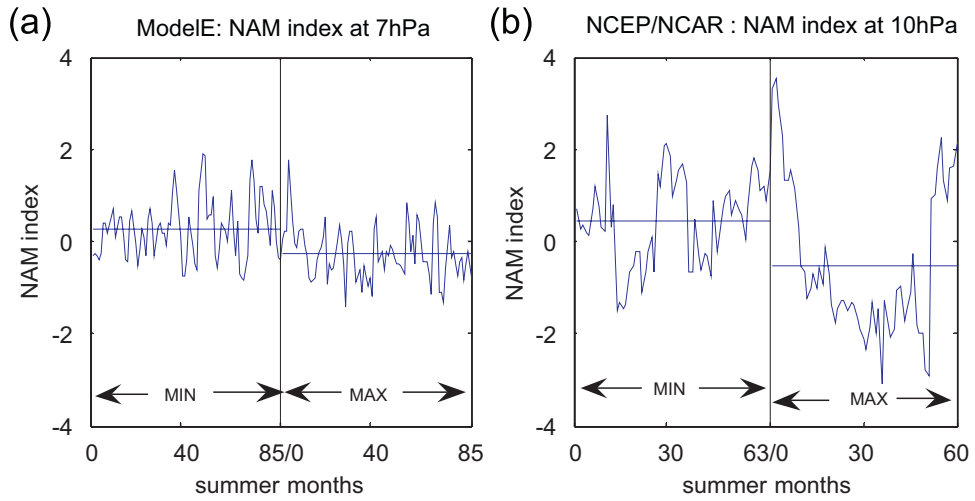

Fig. 4. NAM index for summer (from May to September) for (a) GISS ModelE MIN/MAX run at 7 hPa (left) and (b) NCEP/NCAR reanalysis at 10 hPa (right) for solar minimum/maximum. The horizontal solid lines represent the mean of each NAM indexes. The MIN/MAX period represents the 17 years of summer (from May to September) from MIN/MAX run for (a) the model and 63 months/60 months of solar minimum/maximum months grouped by the monthly mean UV flux below/above standard deviation from the mean during 1948–2004 for (b) NCEP/NCAR reanalysis.

Table 1
The Student t-test statistics for the significance of the difference between the two means: the mean of the principal components in MAX and the mean of the principal components in MIN

	ModelE (MAX, MIN)	NCEP/NCAR (MAX, MIN)
Standard deviation, σ	0.60 (0.56, 0.64)	1.35 (1.65, 0.97)
Difference between the mean, $\mu_{MIN} - \mu_{MAX}$	0.53 (0.26, −0.26)	0.96 (−0.51, 0.44)
Degrees of freedom, $N_{MAX} + N_{MIN} - 2$	168 (85, 85)	121 (60, 63)
t-Value	5.76	3.94

Numbers in parentheses are the statistics for MAX and MIN, respectively.

MAX and MIN (shown in Fig. 5). The composites of the difference fields show the unexpected pattern which has the maximum height anomalies in the pole but not in the low latitudes where the maximum variability exists in the EOF pattern. This is because the geopotential height field itself in the summer stratosphere has a strong meridional gradient and is decreasing with latitudes in the summer stratosphere as seen in Fig. 3. Therefore, the composites of the difference fields show the pattern which has the maximum height anomalies in the pole but not in the low latitudes because the original height is much greater in the high latitudes compared with the low latitudes. Quantifying this difference with respect to the NAM index, it increases from 60 m/100 m in MAX/MIN in the subtropics to 240 m in the polar region when the 7 hPa NAM index changes from the one standard deviation below the mean to the one standard deviation above the mean. This is in good agreement with the corresponding increase from 100 to 230 m found in NCEP/NCAR reanalysis data at 10 hPa level (Lee and Hameed, 2007).

The zonal wind velocities for the low and high NAM conditions are compared for MAX and MIN runs in Fig. 6. There is a strong zonally symmetric easterly circulation with very little deformation during low NAM case. The stronger zonal circulation in low NAM vs. high NAM conditions in both MAX and MIN is consistent with the characteristics found in geopotential height differences as shown in Fig. 5, and with the interpretation that the low NAM regime in the model represents an enhancement of the mean summer circulation, analogous to the result obtained from the NCEP/NCAR reanalysis (Lee and Hameed, 2007). The maximum easterly wind velocity at 7 hPa is about −20 m/s for both MAX and MIN simulations, and the amplitude of NAM variability in the zonal wind velocity is ~5 m/s when the 7 hPa NAM index changes from the one standard deviation below the mean to the one standard deviation above the mean. Both the mean wind field itself and the amplitude of the difference to the NAM variability are comparable to those found in observation. The maximum

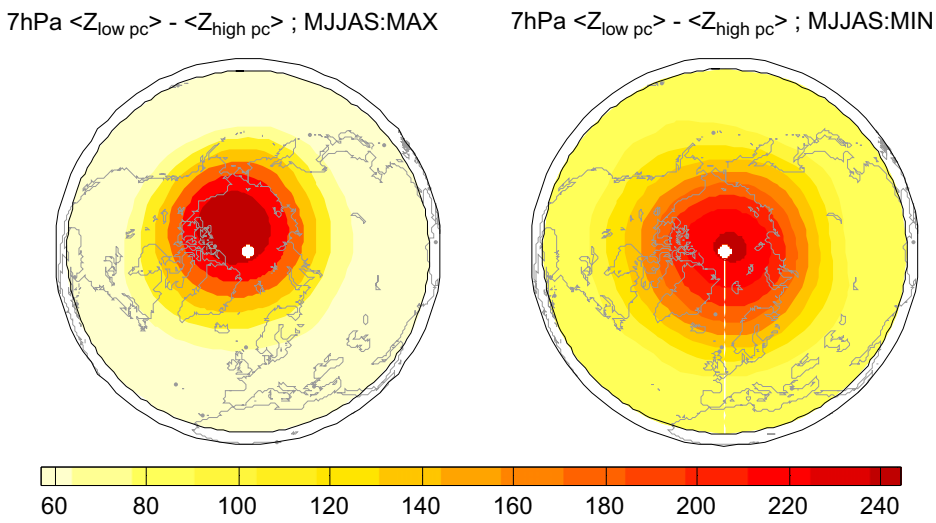

Fig. 5. Composites of summer geopotential height fields difference between low NAM index and high NAM index in m for MAX simulation (left) and MIN simulation (right) at 7 hPa.

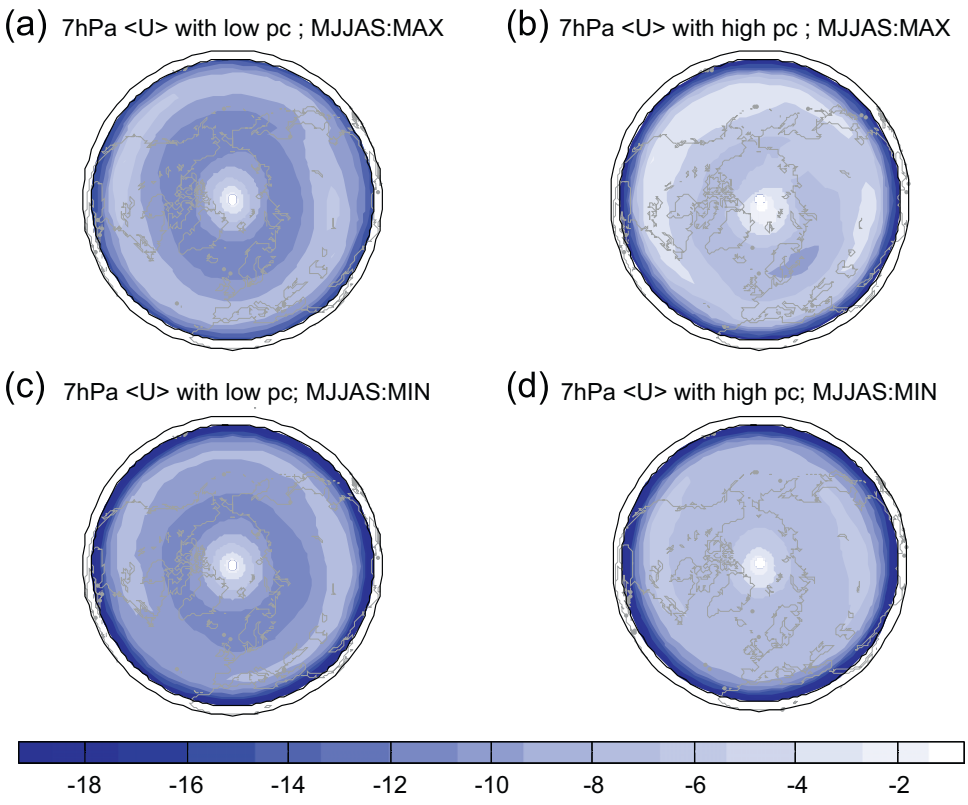

Fig. 6. Composites of zonal wind fields from GISS ModelE MAX and MIN simulation for low NAM index (left) and high NAM index (right) in m/s at 7 hPa from May to September. For the low NAM composites, 11 months for MAX run and 14 months for MIN run are averaged in (a) and (c), respectively. For the high NAM composites, 12 months for MAX run and 16 months for MIN run are averaged in (b) and (d), respectively.

easterly wind velocity is about −25 m/s and the amplitude of NAM variability is 5–10 m/s in the analysis of NCEP/NCAR data at 10 hPa level.

In Fig. 7, the difference of zonal wind velocities at 7 hPa between low and high NAM conditions are compared for MAX and MIN runs, respectively.

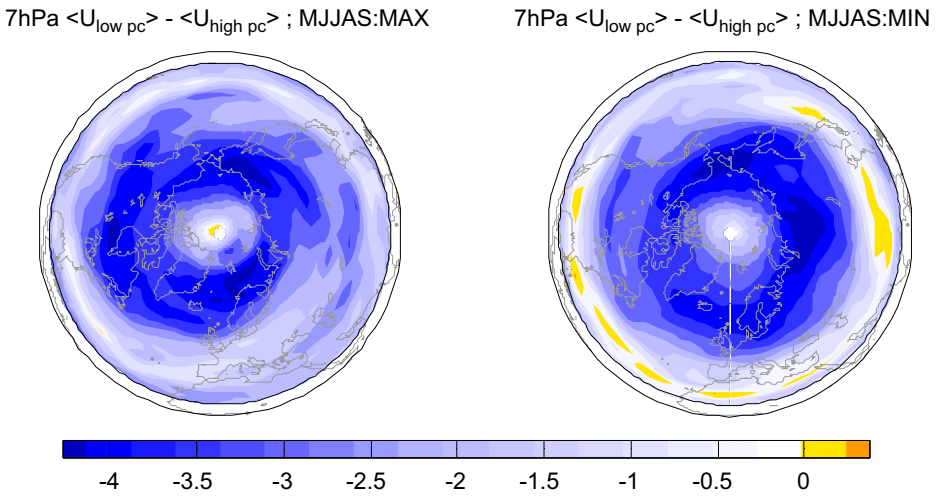

Fig. 7. Composites of summer zonal wind fields difference between low NAM index and high NAM index in m/s for MAX simulation (left) and MIN simulation (right) at 7 hPa.

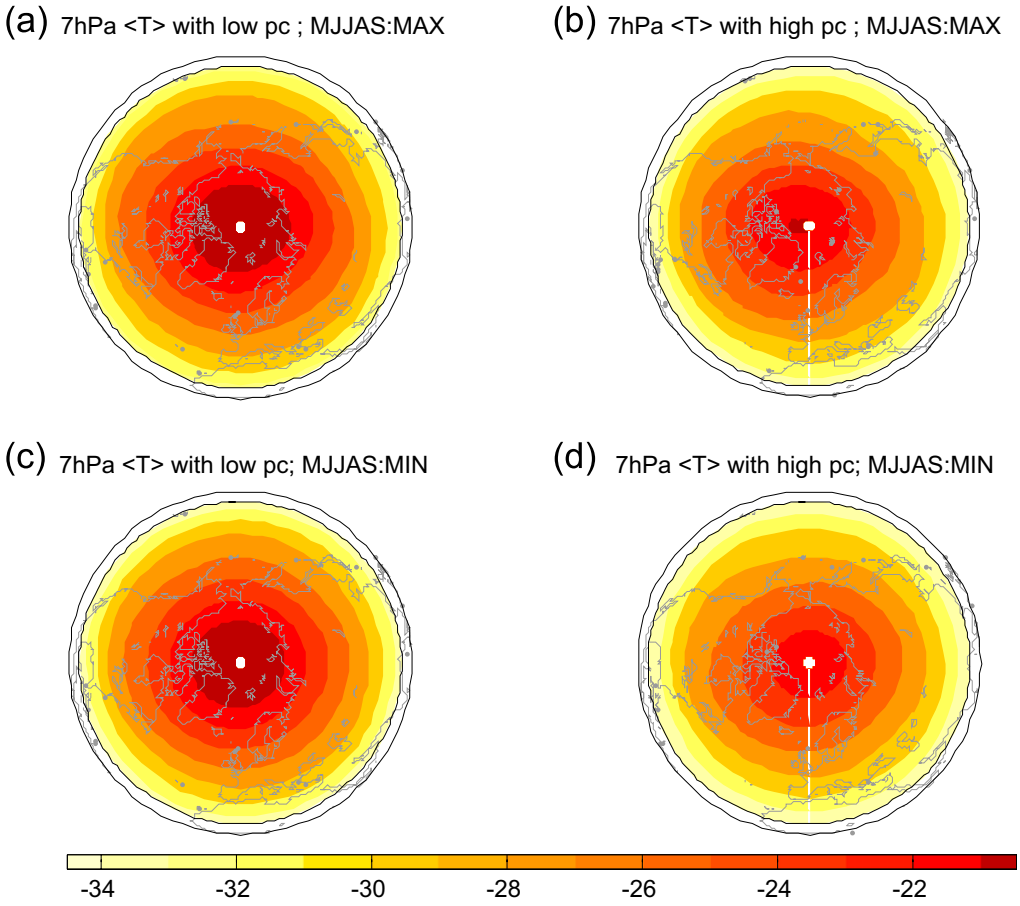

Fig. 8. Composites of summer temperature fields for low NAM index and high NAM index in K for GISS ModelE MAX simulation (left) and MIN simulation (right) at 7 hPa. For the low NAM composites, 11 months for MAX run and 14 months for MIN run are averaged in (a) and (c), respectively. For the high NAM composites, 12 months for MAX run and 16 months for MIN run are averaged in (b) and (d), respectively.

The zonal wind difference shows negative values (more easterly flow) throughout the hemisphere in MAX conditions, while the differences become zero or slightly positive in the tropics in MIN conditions.

Fig. 8 shows the temperature distribution at 7 hPa in low NAM conditions and in high NAM conditions for MAX and MIN simulations, respectively. As shown from NCEP/NCAR reanalysis composites by Lee and Hameed (2007), the temperature is colder during high NAM conditions, especially over the polar region.

Fig. 9 shows the temperature difference at 7 hPa between low and high NAM conditions for MAX and MIN runs. As expected, the temperature difference between two extreme phases is positive in the domain (20–90°N) of summer hemisphere and about 3 K over polar region in both cases. The difference in the tropics is between 0 and 0.5 K in MAX conditions and is between 0.5 and 1.0 K in MIN conditions. This can be anticipated as the geopotential height differences were also greater in solar MIN than in MAX (Fig. 5). The amplitude of the temperature difference appeared in the NCEP/NCAR analysis is 2–5 K throughout the analysis period.

According to the physical interpretation of summer NAM discussed above in Section 5.1, the anti-correlation between the solar flux and the

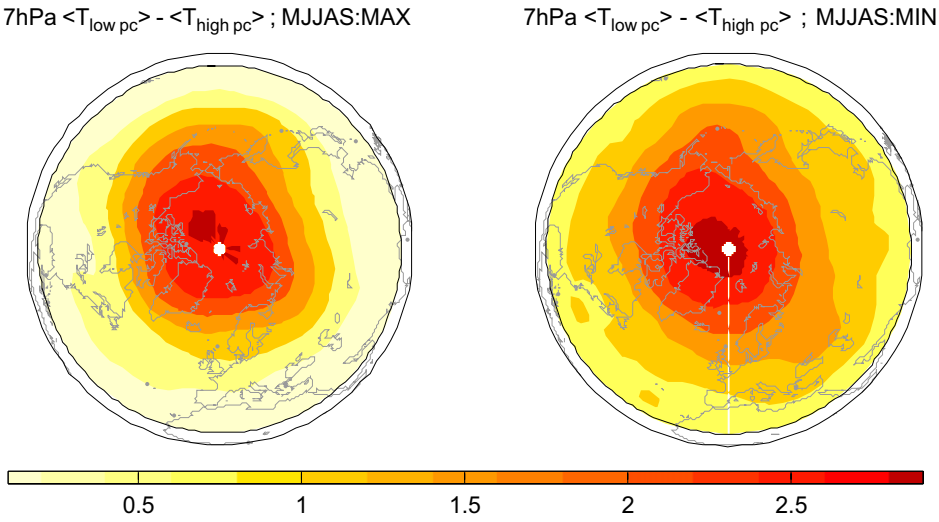

Fig. 9. Composites of summer temperature difference between low NAM index and high NAM index in K for MAX run (left) and MIN run (right) at 7 hPa.

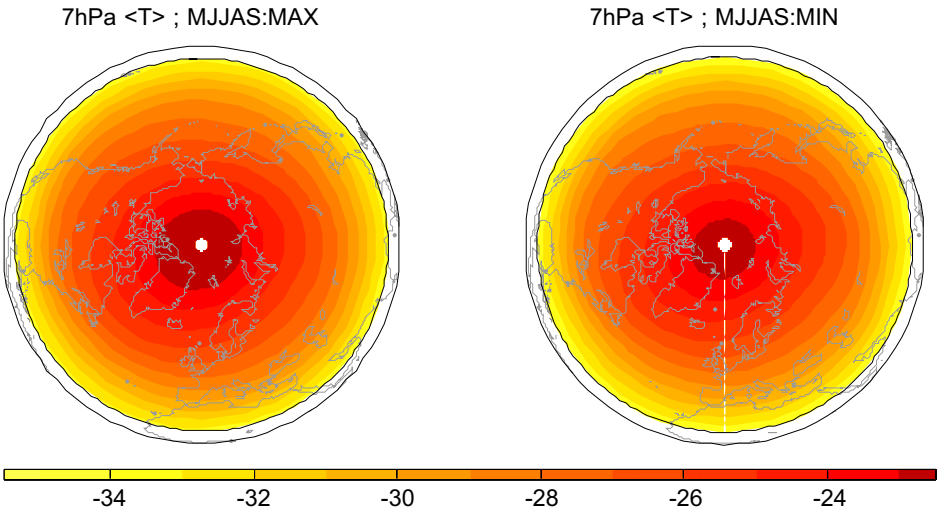

Fig. 10. Composites of ModelE air temperature fields for MAX (left) and MIN (right) runs for 17 years at 7 hPa from May to September. The temperature difference and its statistical significance are discussed in Fig. 11.

NAM suggests that the summer stratosphere is more "summer-like" when the solar activity is near a maximum. This means that the zonal easterly wind flow is stronger and the temperatures are higher than normal. By contrast, low solar activity corresponds to higher NAM conditions in which the stratosphere behaves less "summer-like". This hypothesis is verified from ModelE temperature response to solar UV variability shown in Fig. 10. The average summer hemispheric temperature responses to different solar activity conditions confirm that the summer stratosphere is more "summer-like" when solar UV is stronger. The temperature response to the solar forcing, which is estimated from the difference in the average 7 hPa temperature between MAX and MIN simulation, is 0.6 K in polar region and 0.3 K in midlatitudes except in the middle of Asian continent (Fig. 11). The differences in the temperature are significant throughout the hemisphere at the 95% significant level based on the Student *t*-test, except in the middle of the Asian continent.

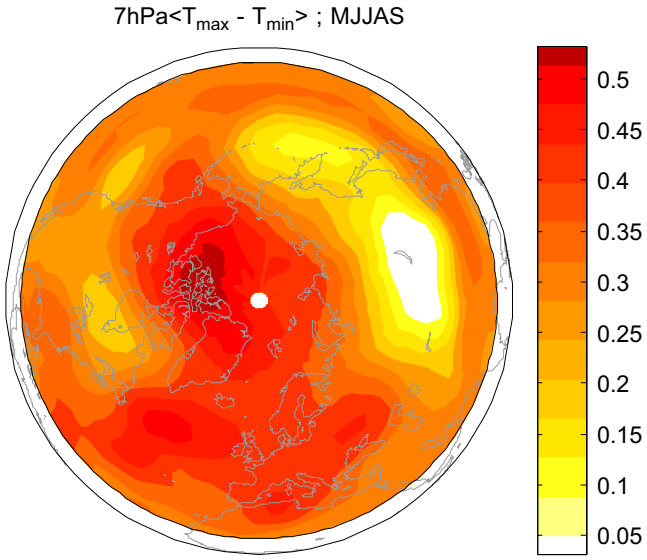

Fig. 11. Composite of temperature difference in K between MAX and MIN runs at 7 hPa. The difference in the temperature is significant throughout the hemisphere at the 95% significant level based on the Student *t*-test, except in the middle of the Asian continent.

5.3. *Response of the summer NAM in the troposphere to solar variability*

We have seen that the summer leading EOF pattern in the lower troposphere has a dipole zonal structure with fluctuations of opposite signs at the high and the midlatitudes (Fig. 2). In the NCEP/NCAR reanalysis, the dominant midlatitude positive center is over the Asian monsoon region, while in the ModelE this center is weaker and shifted to the east. The positive polarity of the NAM index is marked by anomalously low geopotential heights over the polar cap as used conventionally in many studies of the winter NAM (e.g., Thompson and Wallace, 1998, 2000; Fyfe et al., 1999; Shindell et al., 1999, 2001; Miller et al., 2006).

In Fig. 12, the differences of geopotential heights calculated from ModelE simulations at 765 hPa between low and high NAMs are shown in the MAX and MIN. The low NAM mode is marked by anomalously high geopotential heights over the

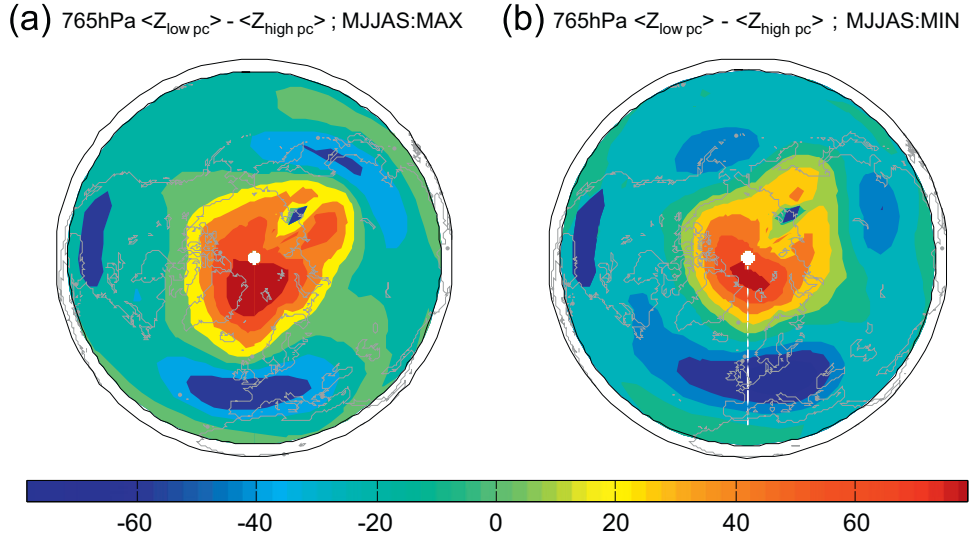

Fig. 12. Composites of ModelE summer geopotential height fields difference between low NAM index and high NAM index in m for (a) MAX run (left) and (b) Min run (right) at 765 hPa.

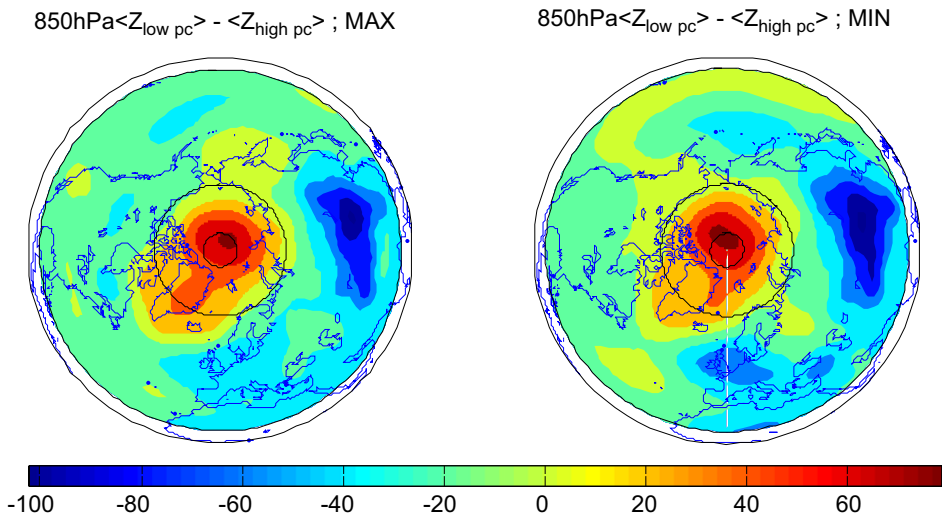

Fig. 13. Composites of NCEP/NCAR summer geopotential height fields difference between low NAM index and high NAM index in m for solar maximum (left) and solar minimum (right) at 850 hPa.

polar region and by anomalously low heights in the zonal belt centered near 45°N. The signal of NAM in MIN (80 m) is greater in northern Europe than in MAX (50 m). As in the EOF pattern in Fig. 2, the signal of NAM in ModelE simulation over Asian continent differ from that in the NCEP/NCAR reanalysis at lower troposphere. In the solar maximum conditions, the pronounced NAM signal in geopotential heights is over the eastern coasts of Asia. In the solar minimum conditions, it is divided into two centers, one over the Aleutian Island region and the other over Siberia.

To compare this NAM signal in the ModelE with that in the observation, we have classified the NCEP/NCAR reanalysis geopotential heights at 850 hPa into high and low NAM index cases as in the ModelE, and then further categorized for solar maximum and solar minimum using the monthly mean UV flux. The high/low solar activity months are sampled as those in which its UV flux is above/below one standard deviation from the mean of already selected high NAM or low NAM cases. The results for the differences in the geopotential heights between low and high NAM composites are shown in Fig. 13 for solar maximum and solar minimum conditions. We notice that the geopotential heights over the Asian monsoon region are lower by more than 50 m and they are higher by more than 50 m in the Arctic regions in low NAM condition. The difference composites between the solar maximum and minimum conditions are qualitatively similar. However, consistent with the model, the composite geopotential height differences in reanalysis show that the two negative anomalies in Euro-Atlantic and Aleutian island regions are enhanced in the solar minimum conditions.

6. Conclusions

The leading EOFs of summer geopotential heights, or the northern annular modes (NAMs), obtained from the GISS ModelE in the stratosphere and troposphere reproduce salient features of the corresponding patterns obtained from NCEP/NCAR reanalysis data. The model simulated pattern in the stratosphere is consistent with the interpretation that the low values of its principal component represent a regime of above-normal summer conditions, i.e., the distribution of the geopotential heights, zonal winds and temperatures have positive anomalies with respect to the mean summer state. Similarly, the high NAM regime conditions represent a less summer-like state. The NAM in the troposphere is dominated by variability over the Asian monsoon region, but the monsoon pattern in the ModelE is weaker and shifted to the east in comparison with that obtained from the NCEP/NCAR reanalysis. The ModelE simulations produced incoherent EOF patterns near the surface presumably due to problems with parameterization of boundary layer processes. Comparing model simulations in the solar maximum and in the solar minimum conditions, we find that the summer stratosphere has positive anomalies with respect to the average summer conditions under maximum conditions, i.e., it is more summer-like than the average summer state,

while it is less summer-like than the average state in solar minimum conditions. This response is similar to that in the NCEP/NCAR reanalysis. Consistent with its interpretation, the NAM index values are lower in solar maximum conditions than in the minimum conditions. Furthermore, the variability in atmospheric conditions associated with the NAM is greater in solar minimum conditions than in maximum conditions in the model.

The NAM in the lower troposphere contains only about 16% (in the NCEP/NCAR reanalysis) to 18% (in the model) of the variance in geopotential heights. This may be a reason why our comparison of composite differences between low and high NAM for solar minimum and maximum conditions in the lower troposphere did not yield significant differences in the model simulation or in the NCEP/NCAR reanalysis.

The comparisons presented in this paper highlight two areas where improvements in ModelE can result in significantly more realistic simulations. One is the lack of coherence in the EOF patterns below 765 hPa, which may indicate an unrealistically high heterogeneity in boundary layer fluxes. The other is the weakness of the simulated Asian monsoon and its displacement to the east in comparison with observations. The largest geopotential height variability in the leading EOF in the lower troposphere is in the monsoon region, and its incorrect simulation therefore indicates possible distortions in the simulation of regional climate pattern in Asia. Similarity of the simulated NAMs in the middle and upper troposphere and in the stratosphere with the patterns found in the NCEP/NCAR reanalysis, and their responses to changes in solar activity is an encouraging result. Given these basic agreements, further comparative analysis seems useful to identify important sun–climate mechanisms driving climatological changes. An important future work along these lines would be to investigate and to compare the responses of the ozone distribution to variations in NAM and in solar activity. Another topic to investigate is how complete the reaction scheme in the chemistry model should be in order to adequately simulate the ozone response necessary for a realistic thermal and dynamic response in the stratosphere.

Acknowledgment

This work was supported by NASA's Living with a Star Program and the Atmospheric Chemistry Modeling and Analysis Program.

References

Baldwin, M.P., Dunkerton, T.J., 2001. Stratospheric harbingers of anomalous weather regimes. Science 294, 581–584.

Charney, J.G., Drazin, P.G., 1961. Propagating of planetary-scale disturbances from the lower into the upper atmosphere. Journal of Geophysical Research 66, 83–109.

Fyfe, J.C., Boer, G.J., Flato, G.M., 1999. The arctic and Antarctic oscillations and their projected changes under global warming. Geophysical Research Letters 26, 1601–1604.

Geller, M., 2006. Discussion of the solar UV/planetary wave mechanism. Space Science Reviews 125, 237–246.

Kalnay, E., et al., 1996. The NCEP/NCAR 40-year reanalysis project. Bulletin of the American Meteorological Society 77, 437–471.

Lean, J., 2000. Evolution of the Sun's spectral irradiance since the Maunder Minimum. Geophysical Research Letters 27, 2425–2428.

Lee, J.N., Hameed, S., 2007. The Northern Hemisphere annular mode in summer: its physical significance and its relation to solar activity variations. Journal of Geophysical Research 112, D15111.

Miller, R.L., Schmidt, G.A., Shindell, D.T., 2006. Forced annular variations in the 20th century Intergovernmental Panel on climate change fourth assessment report models. Journal of Geophysical Research 111, D18101.

Schmidt, G.A., Ruedy, R., Hansen, J.E., Aleinov, I., Bell, N., Bauer, M., Bauer, S., Cairns, B., Canuto, V., Cheng, Y., Del Genio, A., Faluvegi, G., Friend, A.D., Hall, T.M., Hu, Y., Kelley, M., Kiang, N.Y., Koch, D., Lacis, A.A., Lerner, J., Lo, K.K., Miller, R.L., Nazarenko, L., Oinas, V., Perlwitz, Ju., Rind, D., Romanou, A., Russell, G.L., Sato, M., Shindell, D.T., Stone, P.H., Sun, S., Tausnev, N., Thresher, D., Yao, M.-S., 2006. Present day atmospheric simulations using GISS ModelE: comparison to in-situ, satellite and reanalysis data. Journal of Climate 19, 153–192.

Shindell, D.T., Miller, R.L., Schmidt, G.A., Pandolfo, L., 1999. Simulation of the recent northern winter climate trends by greenhouse forcing of a stratospheric model. Nature 399, 452–455.

Shindell, D.T., Schmidt, G.A., Miller, R.L., Rind, D., 2001. Northern Hemisphere winter climate response to greenhouse gas, ozone, solar, and volcanic forcing. Journal of Geophysical Research 106, 7193–7210.

Shindell, D.T., Faluvegi, G., Unger, N., Aguilar, E., Schmidt, G.A., Koch, D., Bauer, S.E., Miller, R.L., 2006a. Simulations of preindustrial, present-day, and 2100 conditions in the NASA GISS composition and climate model G-PUCCINI. Atmospheric Chemistry and Physics 6, 4427–4459.

Shindell, D.T., Faluvegi, G., Miller, R.L., Schmidt, G.A., Hansen, J.E., Sun, S., 2006b. Solar and anthropogenic forcing of tropical hydrology. Geophysical Research Letters 33, L24706.

Thompson, D.W.J., Wallace, J.M., 1998. The Arctic Oscillation signature in the wintertime geopotential height and temperature fields. Geophysical Research Letters 25, 1297–1300.

Thompson, D.W.J., Wallace, J.M., 2000. Annular modes in the extratropical circulation. Part I: month-to-month variability. Journal of Climate 13, 1000–1016.

Wagner, R.E., Bowman, K.P., 2000. Wavebreaking and mixing in the Northern Hemisphere summer stratosphere. Journal of Geophysical Research 105, 24,799–24,800.